DOI: 10.1002/chem.200500283

Tunable Charge Delocalization in Dinickel Quinonoid Complexes

Olivier Siri,[a] Jean-philippe Taquet,[a] Jean-Paul Collin,[b] Marie-Madeleine Rohmer,[c] Marc Bénard,[c] and Pierre Braunstein*[a]

Dedicated to Professor Heinrich Vahrenkamp on the occasion of his 65th birthday

Abstract: When a 2,5-diamino-1,4-benzoquinonediimine $C_6H_2(=NR)_2(NHR)_2$ (**2**) is used as a bridging ligand, new dinickel(II) complexes [(acac)Ni{μ-$C_6H_2(=NPh)_4$}Ni(acac)] (**3a**: R = Ph) and [(acac)Ni{μ-$C_6H_2(=NCH_2tBu)_4$}Ni(acac)] (**3b**: R = CH_2tBu) are obtained; upon one-electron oxidation of these complexes delocalized mixed-valence compounds are formed. An X-ray diffraction study on **3b** reveals equalization of the bond lengths within each of the ligand 6π systems and a lack of conjugation between them. The oxidized state in $\mathbf{3b}^+$ involves both the bridging quinonoid ligand and the metal centers, with a major contribution coming from the bridging ligand. Electrochemical and spectroscopic methods were used to study the influence of the N-substituents of the tetranitrogen donor ligands **2**. In this combined experimental and theoretical (DFT) study, it is also shown that the electronic structure within the dinickel system can be altered by addition of a coordinating ligand such as pyridine. The latter favors the high-spin configuration with semi-occupied metal-centered orbitals, leading to a metal–metal interaction in the mixed-valence Ni^{II}–Ni^{III} $\mathbf{3b}^+$ system.

Keywords: coordination modes · density functional calculations · metal–metal interactions · mixed-valence compounds · N ligands

Introduction

The concept of noninnocent ligands in coordination chemistry has usually been employed to determine whether the odd electron on a paramagnetic species is ligand or metal centered.[1] Dinuclear complexes in which the odd electron is located on the metal may display electronic communication depending on their bridging ligand, and this feature is central to the emergence of new properties in biological, physical, and chemical systems.[2] More than 35 years after the pioneering studies on the Creutz–Taube diruthenium complex containing a pyrazine (or related) bridging ligand, which provided the first example of an interaction between two metal centers mediated by an organic linker,[3] considerable research effort is still dedicated to the study of electronic communication between transition metal centers, which is of fundamental importance for the design of molecular-based electronic devices.[4] Linkers used to mediate the electron transfer between the redox centers should provide effective overlap between their π systems and the orbitals of the metals.[2,5]

The situation in which the odd electron is located on the bridging ligand gives rise to noninnocent behaviour.[4d] Organometallic compounds containing radical ligands are attracting increasing interest in many areas of science, ranging from bioinorganic chemistry to solid-state physics.[6] Chelating 1,2-dioxolenes (type **1**) have recently attracted much attention as spacers because they combine ligand-based and metal-based redox activity.[7] Extending such studies to their

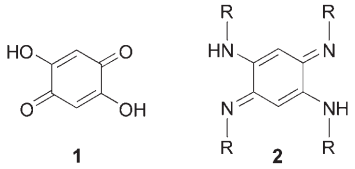

[a] Dr. O. Siri, J.-p. Taquet, Dr. P. Braunstein
Laboratoire de Chimie de Coordination, UMR 7513 CNRS
Université Louis Pasteur, 4, rue Blaise Pascal
67070 Strasbourg Cedex (France)
Fax: (+33) 390-241-322
E-mail: braunst@chimie.u-strasbg.fr

[b] Dr. J.-P. Collin
Laboratoire de Chimie Organo-Minérale, UMR 7513 CNRS
Université Louis Pasteur, 4, rue Blaise Pascal
67070 Strasbourg Cedex (France)

[c] Dr. M.-M. Rohmer, Dr. M. Bénard
Laboratoire de Chimie Quantique, UMR 7551 CNRS
Université Louis Pasteur, 4, rue Blaise Pascal
67070 Strasbourg Cedex (France)

nitrogen analogues $C_6H_2(=NR)_2(NHR)_2$ (**2**)[8,9] would allow further electronic fine-tuning, because the NR group should not only directly affect the metal coordination, but also allow variations of the R substituents.

The first and only dinuclear complex prepared from a 2,5-diamino-1,4-benzoquinonediimine derivative **2** (in which $R = CH_2tBu$, see **2b**) was a diplatinum(II) compound, isolated in approximately 15% yield, which limited considerably its study.[8a] Here we describe the high yield synthesis and properties of new dinickel(II) complexes obtained from **2** of which the monoxidation products $\mathbf{3}^+$ have been investigated experimentally and theoretically, also in the presence of pyridine. The influence of the N-substituents on the redox behaviour of **3a**,**b** has also been clearly demonstrated.

Results and Discussion

Synthesis and characterization: The metalation of azophenine $C_6H_2(=NPh)_2(NHPh)_2$ (**2a**)[9] with $[Ni(acac)_2]$ (2 equiv) in THF (Scheme 1) afforded $[(acac)Ni\{\mu\text{-}C_6H_2(=NPh)_4\}Ni(acac)]$ (**3a**) as a violet crystalline solid (ca. 82% yield).

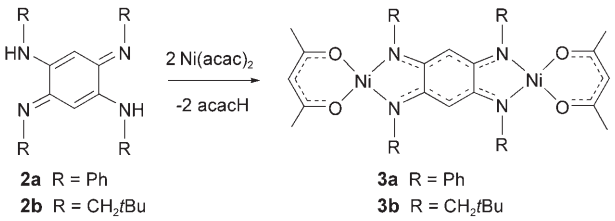

Scheme 1. Synthesis of the dinuclear complexes **3a** and **3b**.

The ^1H NMR spectrum of **3a** revealed the presence of four magnetically equivalent methyl groups and no NH resonance. This is consistent with a bis-chelating, tetradentate behaviour for the dianionic ligand derived from **2a** and with a fully delocalized π system. This prompted us to study the ability of **3a** to display ligand-mediated metal–metal interactions. The strongly σ donor N_2O_2 ligand set around each Ni^{II} center is favorable for an oxidation process occurring mostly at the metal, although related systems can display noninnocent character.[5b]

The electronic spectrum of **3a** shows two transitions at 520 and 553 nm in THF (Figure 1), typical of a $\pi\rightarrow\pi$ transition of the benzoquinonediimine bridging ligand[8b] and of a MLCT transition,[5a] respectively. A weaker absorption is observed around 650 nm, which could be assigned to the HOMO→LUMO allowed transition (of LMCT character) calculated to be of weak intensity (see below).

The cyclic voltammogram of **3a** shows two poorly reversible redox waves at 0.15 and 0.45 V versus Fc^+/Fc resulting from two successive one-electron oxidation processes (anhydrous CH_2Cl_2, $N(nBu)_4PF_6$ as supporting electrolyte; Figure 2).

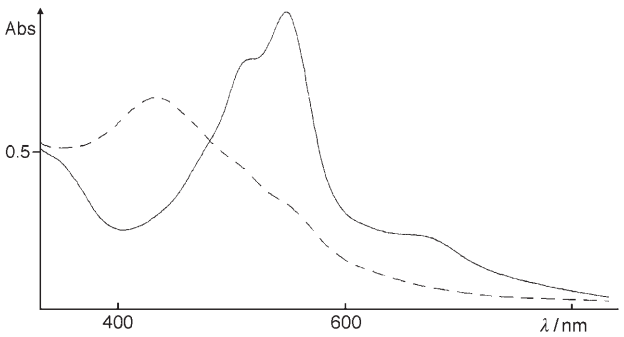

Figure 1. Electronic spectra of **3a** (——) and the mixed-valence complex $\mathbf{3a}^+$ (– – –), recorded in THF at room temperature

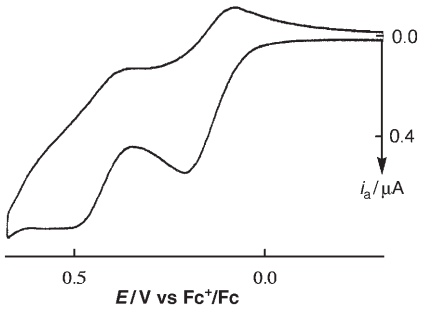

Figure 2. Cyclic voltammogram of **3a** in anhydrous CH_2Cl_2 (0.1 M $N(nBu)_4PF_6$) at a scan rate of 100 mV s^{-1}.

Owing to the proximity of the second oxidation wave ($\Delta E_{1/2} = 300$ mV), attempts to generate pure $\mathbf{3a}^+$ by controlled potential electrolysis ($E_{applied} = 0.43$ V vs Fc^+/Fc) in dry THF failed (as indicated by excessive current consumption). However, the absorption bands of **3a** at 520 and 553 nm were clearly replaced by a single, broad band at 438 nm for $\mathbf{3a}^+$ (Figure 1). No intervalence transfer band was observed at room temperature in the NIR region, which could be due to a too low concentration of $\mathbf{3a}^+$ (see above) and/or an intrinsically weak band.[10]

The π-acceptor N-substituent in **3a** was then replaced by a σ-donor group, which should stabilize a formally $[Ni^{II}\text{–}Ni^{III}]^+$ species, and $[(acac)Ni\{\mu\text{-}C_6H_2(=NCH_2tBu)_4\}Ni(acac)]$ (**3b**) was prepared in toluene by metalation of **2b**, similarly to **3a** (Scheme 1). An X-ray diffraction study confirmed the centrosymmetry of the molecule (Figure 3). The dianion derived from **2b** acts as a tetradentate bridging ligand in a bis(chelating) fashion.

The geometry about the metals is square planar with the nickel atoms being only slightly out of the plane containing the C_6 ring (inter planar deviation angle is $\theta = 23°$; Figure 3).

The Ni···Ni separation of 7.62(2) Å is slightly shorter than that found in a dinuclear nickel complex containing ligand **1**.[11b] By comparison with the bonding parameters in related systems,[8a,b] the similarity of the bond lengths within the N1-C3-C1′-C2′-N2′ and N2-C2-C1-C3′-N1′ moieties is consistent with an extensive electronic delocalization, but there is no

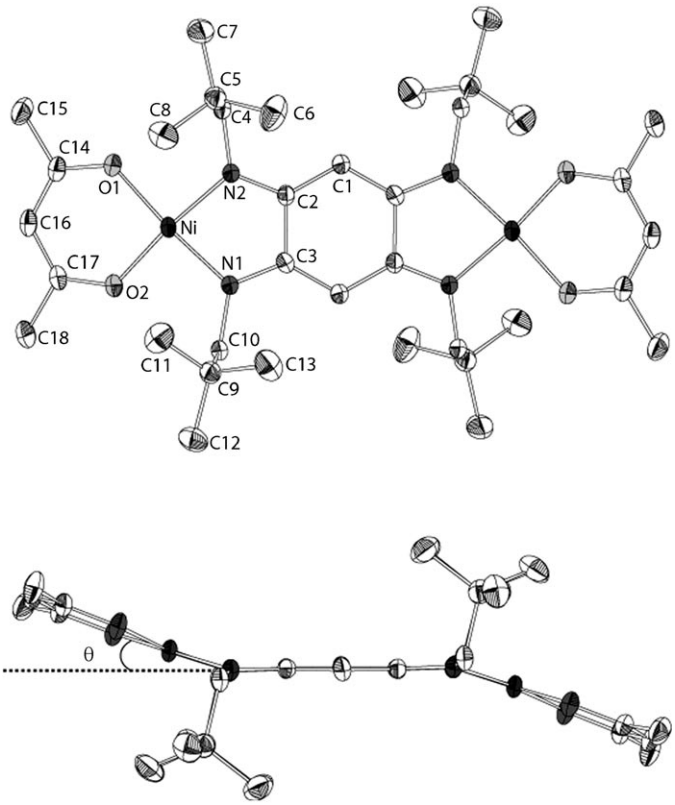

Figure 3. Top and side views of the structure of **3b**. Selected bond lengths [Å] and angles [°]: Ni–N1 1.876(2), Ni–O2 1.848(2), Ni–O1 1.852(2), Ni–N2 1.877(2), N1–C3 1.332(3), C3–C2 1.500(3), C2–C1 1.404(3), C2–N2 1.333(3); N1-Ni-N2 83.27(8), N1-Ni-O1 175.10(7), N1-Ni-O2 91.01(7), O1-Ni-O2 93.84(7), Ni-N1-C3 114.2(2), N2-C2-C3 112.0(2), N1-C3-C2 111.7(2), N2-C2-C1 128.7(2).

conjugation between these two 6π systems, since the C2–C3 distance corresponds to a typical single bond.[8a]

The cyclic voltammogram of **3b** shows two reversible redox processes at 0.05 V and 0.91 V versus Fc^+/Fc (Figure 4), corresponding to a one-electron transfer as demonstrated by coulometry and linear sweep voltammetry. As expected, the more electron rich **3b** is easier to oxidize than **3a** (0.05 vs 0.15 V). The ratio of the peak currents (I_{p_a}/I_{p_c}) is

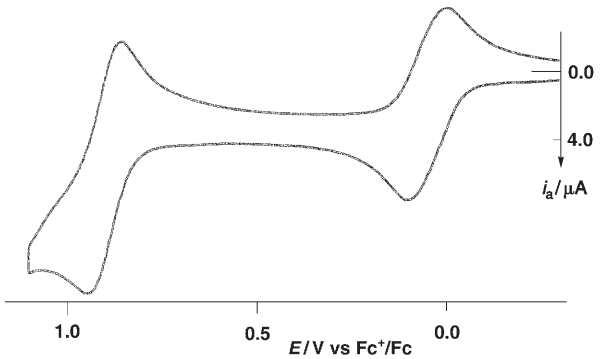

Figure 4. Cyclic voltammogram of **3b** in anhydrous CH_2Cl_2 (0.1 M N-(nBu)$_4$PF$_6$) at a scan rate of 100 mV s^{-1}.

unity and the peak separation ($E_{p_a}-E_{p_c}$) is around 80 mV at different scan rates for each signal. Furthermore, the separation between the two redox processes $\Delta E_{1/2}=850$ mV for **3b** is much larger than for **3a**. This indicates a much higher stability of $\mathbf{3b}^+$ relative to $\mathbf{3a}^+$; this stability originates from the N-substituents (σ-donor alkyl vs π-acceptor aryl groups).

Similarly to **3a**, the electronic spectrum of **3b** at room temperature shows two bands at 479 and 510 nm in CH_2Cl_2 (Figure 5), that can be assigned to a $\pi\rightarrow\pi^*$[8a] and a MLCT transition,[5a] respectively. In the electronic spectrum of $\mathbf{3b}^+$, generated by controlled potential electrolysis ($E_{applied}=0.5$ V vs Fc^+/Fc) in dry CH_2Cl_2, these bands are red shifted at 512 and 542 nm, whereas a blue shift was observed when going from **3a** to $\mathbf{3a}^+$.

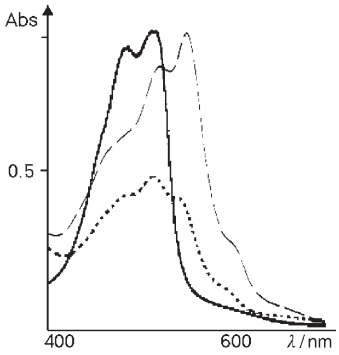

Figure 5. Electronic spectra of **3b** (——), the mixed-valence complex $\mathbf{3b}^+$ without (– – –) and with presence of pyridine (-----), recorded in CH_2Cl_2 at room temperature.

Thus, although the π system in ligand **2a** could be more extended than in **2b** owing to the possible participation of the *N*-phenyl substituents,[8c] a situation which is also observed in their Ni^{II} complexes **3a** and **3b**, the reverse appears to apply to their oxidized species $\mathbf{3a}^+$ and $\mathbf{3b}^+$, respectively. The NIR spectrum (1000–3000 nm) of $\mathbf{3b}^+$, recorded at room temperature during a coulometry experiment, displays a weak band at 1030 nm and a weaker one at 910 nm (Figure 6) that could originate from MLCT or $\pi(d\pi)\rightarrow\pi^*(d\pi)$ transitions in the metal–ligand–metal core.[5d]

With the hope to stabilize an oxidized Ni^{II}–Ni^{III} species by addition of a σ-donor ligand, the behaviour of **3b** was examined in the presence of pyridine. Its electronic spectrum was unaffected, which is consistent with the electrochemical data

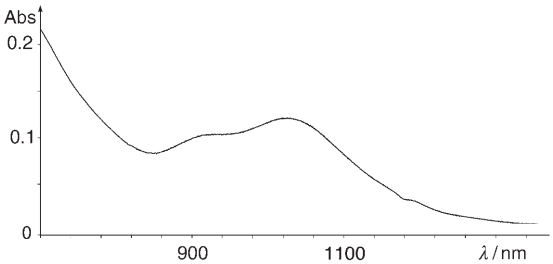

Figure 6. NIR spectrum of $\mathbf{3b}^+$ recorded in CH_2Cl_2 at room temperature.

and theoretical studies (see below) and indicate the lack of coordination of pyridine to the Ni^{II} centers. In contrast, the electronic spectrum of **3b**$^+$ displays three absorptions at 473(sh), 510, and 538 nm (sh), in agreement with coordination of the pyridine to the formally Ni^{III} center (Figure 5). The reversibility of the first wave of the redox process in the cyclic voltammetry of **3b** was not affected by the addition of pyridine, indicating that the latter does not coordinate on the timescale of this experiment. The second oxidation process could not be analyzed, probably because of the instability of the doubly oxidized complex in basic medium. However, after exhaustive electrolysis in the presence of pyridine to generate the mixed-valence species **3b**$^+$, a new reversible redox wave was observed at 0.44 V versus Fc^+/Fc. It is tentatively assigned to the oxidation of the remaining Ni^{II} center, now easier than in the absence of pyridine.

Only an EPR study could determine whether the odd electron on the oxidized species **3b**$^+$ is located more on the ligand or the metal centers. Its spectrum, generated as indicated above in dry THF under N_2 and in the presence of a drop of anhydrous pyridine showed at 4 K two broad signals corresponding to $g_{\parallel} = 2.13$ and $g_{\perp} = 4.16$. These values are characteristic of a spin $S = 3/2$ system in which a low-spin Ni^{III} ($S = 1/2$) would be ferromagnetically coupled to an octahedral Ni^{II} ($S = 1$).[11a] Unfortunately, no hyperfine coupling to the nitrogen atoms (^{14}N) could be observed.[11a] When the EPR spectrum of **3b**$^+$ was recorded at 100 K, a signal at $g \approx 2$ was observed, indicating another coupling scheme. Related temperature-dependent EPR behaviour has been noted in other dinickel systems.[11a] In the absence of pyridine, a signal at $g = 2.028$ ($\Delta\nu_{1/2} = 24$ G) was observed at 4 and 100 K, suggesting a strong ligand involvement and a noninnocent behavior of the bridging ligand.

Theoretical Studies

Complex [(acac)Ni{μ-C_6H_2(=NMe)$_4$}Ni(acac)] (3c) and the mono-oxidized species 3c$^+$: DFT calculations have been carried out on a model of **3b**, in which the CH_2tBu groups were replaced by methyl substituents (**3c**). All geometry optimizations were carried out with the ADF program,[12] using the gradient-corrected BP86 functional and Slater-type atomic basis sets. For first-row atoms, the 1s shell was frozen and described by a single Slater function. The neon core of Ni was also modeled by a minimal, frozen Slater basis. The valence shells of all atoms, including the 4s shell of Ni were triple-ζ, whereas the 4p shell of Ni was described by a single orbital. These sets were supplemented with one polarization function for all non-metal atoms. For the TD-DFT estimate of transition energies, the B3LYP hybrid functional was preferred and the calculations were carried with GAUSSIAN-98,[13] using the previously optimized geometries. For the neutral model complex **3c**, a bent structure similar to that of Figure 3 (C_{2h} symmetry) was used as trial geometry, but the lowest energy for the Ni^{II}–Ni^{II} complex was obtained with a fully planar structure (D_{2h} symmetry). Apart from the θ angle, the main geometrical parameters are accurately reproduced by the calculations (Table 1). The sequence of frontier orbitals is displayed in Figure 7.

Table 1. Electronic configuration, total bonding energies [eV] and selected interatomic distances [Å] observed for **3b** (in italics) and calculated for the closed-shell ground state of **3c**, and for various oxidized species.[a]

	3b	**3c**	**3c**$^+$	[**3c**(py)$_4$]$^+$	[**3c**(py)$_2$]$^+$	[**3c**(py)$_2$]$^+$
energy [eV][b]		−282.611	−276.652	−557.567	−417.096	−416.931
symmetry	C_{2h}	D_{2h}	D_{2h}	D_{2h}	C_{2h}	C_{2h}
Ni–N	*1.876*	1.871	1.862	1.991	1.905	1.891
Ni–O	*1.850*	1.838	1.835	1.988	1.905	1.886
N–C2	*1.332*	1.337	1.335	1.332	1.339	1.337
C2–C3	*1.500*	1.470	1.466	1.486	1.472	1.467
C1–C2	*1.404*	1.405	1.407	1.407	1.405	1.409
O_{acac}–C		1.285	1.287	1.279	1.282	1.285
Ni–N_{py}				2.207	2.246	2.606

[a] **3c**$^+$(doublet ground state) [**3c**(py)$_4$]$^+$ (quartet ground state); [**3c**(py)$_2$]$^+$ (doublet ground state and first excited doublet state). The bonding energy computed for a free pyridine molecule is −70.008 eV. [b] Electronic configurations of the calculated species: **3c**: ground state $^1A_{1g}$ $(a_{1g})^2(b_{3u})^2(b_{1u})^2(b_{3g})^2$; **3c**$^+$: ground state $^2B_{3g}$ $(a_{1g})^2(b_{3u})^2(b_{1u})^2(b_{3g})^1$; [**3c**(py)$_4$]$^+$: ground state $^4B_{1g}$ $(a_{1g})^1(b_{3u})^1(b_{1u})^2(b_{3g})^2(b_{2u})^1$; [**3c**(py)$_2$]$^+$: ground state ^2B_u $(a_g)^2(b_u)^1(a_u)^2(b_g)^2$; [**3c**(py)$_2$]$^+$: excited state ^2B_g $(a_g)^2(b_u)^2(b_u)^2(b_g)^1$.

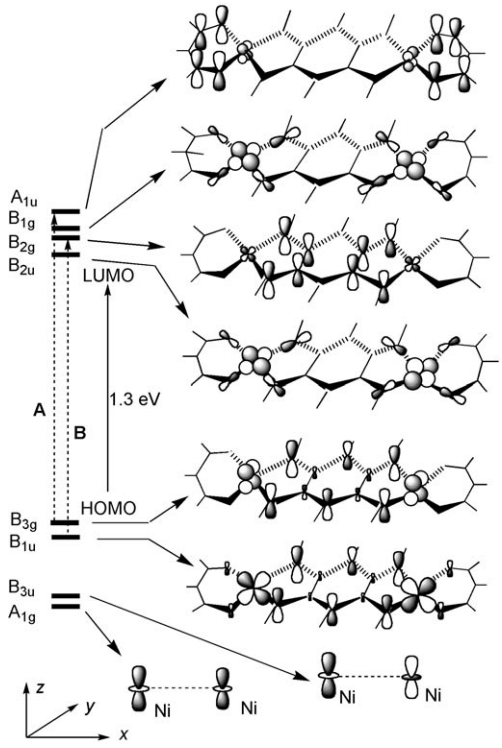

Figure 7. Sequence of frontier orbitals of **3b**, in which the CH_2tBu substituents have been replaced by methyl groups (**3c**).

Following the order of increasing energies, we find: 1) the quasi-degenerate in-phase and out-of-phase combinations of the Ni d_{z^2} orbitals ($18a_{1g}$, $17b_{3u}$); 2) orbital $7b_{1u}$ (48% metal) at 0.8 eV above the d_{z^2} combinations; and 3) the HOMO $5b_{3g}$ (20% Ni vs 72% delocalized over the benzoquinonediimine π-system), separated from $7b_{1u}$ by no more than 0.18 eV. Both the $7b_{1u}$ and the $5b_{3g}$ MOs are the upper terms, mostly ligand-centered, of four-electron π interactions between the metal atoms and the benzoquinonediimine ligand. The major weight of the spacer π system in the metal–ligand antibonding HOMO clearly characterizes benzoquinonediimine as a noninnocent ligand responsible for the highly delocalized character of the unpaired electron in the oxidized complex. Concerning the lowest unoccupied MOs, the LUMO ($14b_{2u}$, 57% Ni) and the LUMO+2 ($13b_{1g}$, 61% Ni) are the in-phase and out-of-phase combinations of the metal d_{xy} orbitals destabilized by the σ donation from the N and O lone pairs. The LUMO+1 of **3c** ($7b_{2g}$) corresponds to the LUMO of the 6π+6π delocalized quinonediimine ligand[6b] with a minor metallic contribution (12%). Finally, the LUMO+3 ($5a_{1u}$) is a π–antibonding combination originating in the acacene ligands with a very small metal contribution (6%) stemming from an out-of-phase combination of the d_{yz} orbitals. The ground state of the oxidized complex $\mathbf{3c}^+$ is obtained by removing one electron from the b_{3g} HOMO. The ionization energy of the isolated molecule is computed to be 5.96 eV, and the main geometrical parameters are practically unaffected with respect to the neutral complex (Table 1), in agreement with the nonbonding character of the HOMO regarding either the benzoquinonediimine spacer or the metal coordination environment (Figure 7).

From the many low-lying singlet excited states characterized from TD-DFT/B3LYP calculations only two are allowed with a significant oscillator strength (*f*). The lowest in energy (transition A in Figure 7) corresponds to the $b_{3g}\rightarrow a_{1u}$ (HOMO→LUMO+3) transition (498 nm and $f=0.076$). Given the weak contribution of Ni to the HOMO, this transition should be considered as a $\pi\rightarrow\pi^*$ excitation, but corresponds to a charge transfer from the benzoquinonediimine to the acacene ligands. Transition B (Figure 7), computed at 450 nm ($f=0.67$) has a MLCT character and mainly corresponds to the $b_{1u}\rightarrow b_{2g}$ excitation (HOMO−1→LUMO+1). In spite of the difference in the computed oscillator strengths, the two broad peaks observed at 510 and 479 nm should be assigned to transitions A and B. However, we cannot ensure that the energy sequence of the observed transitions is correctly reproduced by the calculations. Indeed, it has been recently shown that the energy of the charge-transfer excitations, like transition A, are systematically underestimated by TD-DFT.[14]

Oxidized pyridine adducts $[\mathbf{3c}(py)_4]^+$ and $[\mathbf{3c}(py)_2]^+$: Calculations have also been carried out to predict the behaviour of the neutral and oxidized forms of **3c** in the presence of pyridine. Four-pyridine adducts with octahedral coordination of Ni atoms, D_{2h} symmetry, and with the planes of the heterocycles perpendicular to the plane of the complex and to the Ni–Ni line were considered for **3c** and $\mathbf{3c}^+$ and their geometries optimized. The neutral complex was found to be insensitive to pyridine, as far as a closed-shell electronic configuration is retained: the interaction remains repulsive at a Ni–N distance of 3.0 Å. This is consistent with the UV-visible spectrum of **3b** and its cyclic voltammogram, which are unaffected by the addition of pyridine. No open-shell configuration was considered, since the Ni^{II}–Ni^{II} complex is diamagnetic. However, the approach of the pyridine ligands raises the energy of the nickel d_{z^2} orbital combinations, a_{1g} and b_{3u}, which develop an antibonding interaction with the nitrogen lone pairs. In the oxidized species, an attractive interaction with pyridine was obtained by removing two electrons from these orbitals, one of which was transferred to the LUMO of the complex. The resulting $^4B_{1g}$ quartet state corresponds to the configuration $(b_{1u})^2(b_{3g})^2(a_{1g})^1(b_{3u})^1(b_{2u})^1$. The stabilization of the four pyridine fragments amounts 20.5 kcal mol^{-1} and the Ni–N distance is 2.21 Å. The population of the σ-antibonding b_{2u} orbital yields a stretching of the Ni–N and Ni–O distances by 0.13 and 0.15 Å, respectively (Table 1). The high-spin ground state found for $\mathbf{3c}^+$ in the presence of pyridine agrees well with the interpretation of the EPR spectrum. At variance with $\mathbf{3c}^+$, the $5b_{3g}$ delocalized orbital remains doubly occupied in the pyridine adduct. The magnetic orbitals a_{1g}, b_{3u}, and b_{2u} are mostly metal centered and do not extend beyond the adjacent coordination shell; they should favor a more localized mixed-valence state. Less favorable, low-spin configurations of $[\mathbf{3c}(py)_4]^+$ and other types of association between $\mathbf{3c}^+$ and pyridine are discussed below:

The $(a_{1g})^2(b_{3u})^1(b_{1u})^2(b_{3g})^2$ configuration: In this $^2B_{3u}$ doublet electronic state, only one electron was removed from the Ni–N antibonding MOs and none had to be transferred to a high-lying orbital. The bonding energy stabilizes the four pyridines by 12.6 kcal mol^{-1} only. Since only one electron was removed from the Ni–N antibonding MOs the pyridine moieties remain at a relatively large distance from Ni: 2.45 Å.

The $(a_{1g})^2(b_{3u})^2(b_{1u})^2(b_{3g})^1$ ($^2B_{3g}$) configuration: Both Ni-N antibonding MOs remain doubly occupied, whereas the extra electron is removed from the b_{3g} HOMO of the **3c** complex. At variance with the neutral molecule, the coordination of the pyridine ligands is favoured by 8.6 kcal mol^{-1}, probably owing to the increase of electrostatic attraction. However, the Ni–N_{py} interaction is very weak and the computed Ni–N distance quite long: 2.78 Å.

An alternative to the four-pyridine adduct is a complex in which one pyridine only is attached to each metal, giving rise to a square-pyramidal coordination. The symmetry of the $[\mathbf{3c}(py)_2]^+$ complex becomes C_{2h}. In spite of the pyramidalization that can be expected for the equatorial coordination environment, the behaviour of the frontier MOs is qualitatively the same as in the former case, the major effect of the pyridine approach being a raise of the A_g and A_u

MOs accommodating the metal d_{z^2} electrons. As for the 4-py adduct, three electronic states were considered.

The $(a_g)^1(b_u)^1(b_u)^2(b_g)^2(a_u)^1$ configuration: With two electrons removed from the antibonding Ni–N_{py} MOs and one transferred to the a_u LUMO, this quartet state is electronically equivalent to the ground state of the 4-py adduct. However, in the present case it is nonbonding, with an energy of −416.65 eV, equivalent to the energy of **3c** augmented with that of two isolated pyridine molecules.

The $(a_g)^2(b_u)^1(a_u)^2(b_g)^2$ configuration: In this doublet state, the removed electron originated from one of the Ni–N_{py} antibonding MOs. This electronic configuration should be correlated to the $^2B_{3u}$ doublet state of the 4-py adduct. However, due to the pyramidalized structure at Ni and to the lack of *trans* influence, the Ni–N repulsion is greatly reduced with respect to the D_{2h} structure, so that the Ni–N equilibrium distance contracts to 2.246 Å (Table 1). As a secondary effect of the above-mentioned pyramidalization, the equatorial metal–ligand distances increase by 0.03 and 0.06 Å. This doublet state is the ground state of the 2-py adduct. With a bonding energy equal to 10.3 kcal mol^{-1} for the two pyridines, the stabilization per ligand is the same as for the 4-py adduct. The 2-py stoichiometry could therefore be competitive in case of a convenient tuning of the available amount of pyridine. However, as long as pyridine is in excess, the 4-py adduct is clearly favored.

The $(a_g)^2(b_u)^2(b_u)^2(b_g)^1$ configuration: This doublet configuration is electronically equivalent to state $^2B_{3g}$ of the 4-py adduct. The double occupancy of the two Ni–N_{py} antibonding MOs keeps the pyridine moieties relatively far from the metal (2.606 Å). A stabilization of 6.5 kcal mol^{-1} for the two pyridine ligands is nevertheless associated with this electronic state.

Conclusion

We have reported new dinuclear complexes **3a** and **3b** containing a bridging quinonoid ligand. Compared to aromatic bridging ligands used in related dinuclear systems,[4b] ligands of type **2** have two electrons less; this should favor oxidation at the metal rather than at the ligand. However, the charge delocalization (metal vs ligand)[15] investigated by a combined experimental and theoretical (DFT) study on **3b**$^+$, mostly involves the bridging ligand, which contributes most to the one-electron oxidation of **3**. It is shown that the electronic structure of **3b**$^+$ can be altered by addition of a coordinating ligand such as pyridine, which favors the high-spin configuration with semi-occupied metal-centered orbitals, leading to a metal–metal interaction in the Ni^{II}–Ni^{III} **3b**$^+$ system. In contrast to most previously studied systems,[4d,5a,5c,5e,7] ligands of type **2** allow modifications of the N-substituents, thus making possible fine-tuning of the properties of the corresponding dinuclear complexes, as demonstrated here with **3a** and **3b**. Further variations will therefore become possible. These complexes are furthermore being evaluated as homogeneous catalysts for olefin oligomerization, since dinuclear complexes displaying metal–metal interactions are of growing interest in catalysis.[16]

Experimental Section

General: Analytical-grade reagents were obtained from commercial suppliers and were used directly without further purification. Solvents were distilled under argon prior to use and dried by standard methods. ^{1}H NMR spectra were recorded in $CDCl_3$ and [D_6]DMSO with a AC300 Bruker spectrometer, operating at 300 MHz for ^{1}H spectra. Chemical shifts are reported in ppm relative to the singlet at $\delta = 7.26$ ppm for $CDCl_3$. Splitting patterns are indicated as s, singlet; m, multiplet. Elemental analyses were performed by the "service de microanalyse de L'Institut de Chimie," Strasbourg. FAB mass spectral analyses were recorded on an autospec HF mass spectrometer and EI mass spectral analyses were recorded on a Finnigan TSQ 700. UV/Vis and NIR spectra (absorption spectroscopy) were recorded at room temperature with a Kontron Instruments UVIKON 860 or a Varian Cary 05E spectrophotometer, respectively. The EPR spectra were recorded on a ESP 300 Bruker spectrometer. Electrochemical experiments were performed with a three-electrode system consisting of a platinum working electrode, a platinum wire counter electrode, and a silver wire as pseudo-reference electrode. All potentials are reported versus the ferrocinium/ferrocene couple. The measurements were carried out under Ar, in degassed CH_2Cl_2 (distilled from CaH_2 under N_2), using 0.1 M $N(n\text{Bu})_4PF_6$ as the supporting electrolyte. An EG&G Princeton Applied Research Model 273 A potentiostat connected to a computer (Programme Research Electrochemistry Software) was used for the cyclic voltammetry and potential controlled electrolysis experiments.

Synthesis of [(acac)Ni{μ-C_6H_2(=NPh)$_4$}Ni(acac)] (3a): Ligand **2a**[9] (0.68 mmol, 0.30 g) was dissolved in THF (100 mL) and Ni(acac)$_2$ (1.36 mmol, 0.35 g) was added to the red solution, which turned immediately into intense purple. The reaction mixture was stirred at room temperature overnight. The solution was then filtered through Celite, the filtrate was evaporated, and the solid was redissolved in dichloromethane (100 mL), and slowly evaporated to afford **3a** as a violet crystalline product. Yield: 0.42 g (82 %); ^{1}H NMR (300 MHz, CD_2Cl_2, 298 K): $\delta = 1.35$ (s, 12H; CH_3-acac), 4.34 (s, 2H; N=C=C-H), 5.20 (s, 2H; CH-acac), 7.2 ppm (m, 20H; CH-aryl); ^{13}C{^{1}H} NMR (100 MHz, CD_2Cl_2, 298 K): $\delta = 24.60$ (CH_3-acac), 89.28 (H-*C*=C), 100.90 (CH-acac), 124.52, 126.94, 127.57, (CH-aryl), 145.11 (C-aryl), 165.51 (C=N), 186.21 ppm (C=O); elemental analysis calcd (%) for $C_{40}H_{36}N_4O_4Ni_2$: C 63.71, H 4.81, N 7.43; found: C 63.84, H 5.02, N 7.33; UV-visible (CH_2Cl_2): λ (ε): 523 (16600), 555 nm (19500); MS (Maldi-TOF): m/z: 753.231 $[M+1]^+$.

Synthesis of [(acac)Ni{μ-C_6H_2(=NCH$_2$*t*Bu)$_4$}Ni(acac)] (3b): Ligand **2b**[8] (0.48 mmol, 0.20 g) and Ni(acac)$_2$ (0.96 mmol, 0.25 g) were dissolved in toluene (100 mL) and heated to reflux for one night. The solution was then concentrated and green crystals suitable for an X-ray analysis were isolated by filtration. Yield: 0.19 g (55 %). ^{1}H NMR (300 MHz, $CDCl_3$, 298 K): $\delta = 1.05$ (s, 36H; CH_3), 1.79 (s, 12H; CH_3-acac), 2.11 (s, 8H; N-CH_2), 4.93 (s, 2H; N=C=C-H), 5.34 ppm (s, 2H; CH-acac); ^{13}C{^{1}H} NMR (75 MHz, $CDCl_3$, 298 K): $\delta = 25.45$ (CH_3-acac), 29.00 (C*Me*$_3$), 34.82 (C*Me*$_3$), 51.72 (N-CH_2), 88.13 (H-*C*=C), 101.13 (CH-acac), 167.02 (C=N), 185.86 ppm (C=O); elemental analysis calcd (%) for $C_{36}H_{60}N_4O_4Ni_2$: C 59.21, H 8.28, N 7.67; found: C 59.22, H 8.18, N 7.69; UV-visible (CH_2Cl_2) λ (ε): 479 (13500), 510 nm (14700).

X-ray crystallography: The diffraction data for **3b** were collected on a Nonius Kappa-CCD area detector diffractometer ($Mo_{K\alpha}$, $\lambda = 0.71070$ Å; phi scan). The cell parameters were determined from reflections taken from one set of ten frames (1.0° steps in phi angle), each at 20 s exposure. The structure was solved by using direct methods (SHELXS97) and refined against F^2 by using the SHELXL97 software. The absorption was

corrected empirically (with Sortav).[17] All non-hydrogen atoms were refined with anisotropic parameters. The hydrogen atoms were included in their calculated positions and refined with a riding model in SHELXL97.[18]

Crystal data: $C_{36}H_{60}N_4O_4Ni_2$, $M_r = 730.30\ g\,mol^{-1}$, green prism, size $0.08 \times 0.10 \times 0.13$ mm, triclinic, space group $P\bar{1}$, $a = 9.7060(10)$, $b = 10.2970(10)$, $c = 10.9920(10)$ Å, $\alpha = 63.863(5)$, $\beta = 88.607(5)$, $\gamma = 77.502(5)°$, $V = 959.70(16)$ Å^3, $T = 293$ K, $Z = 1$, $\rho_{calcd} = 1.264\ g\,cm^{-3}$, $\mu(Mo_{K\alpha}) = 1.021\ mm^{-1}$, $F(000) = 392$, 10595 reflections in $h(-13/10)$, $k(-14/14)$, $l(-15/15)$, measured in the range $2.1° \le \theta \le 30.0°$, 5582 independent reflections, $R_{int} = 0.039$, 4207 reflections with $I > 2\sigma(I)$, 208 parameters, $R1_{obs} = 0.0459$, $wR2_{obs} = 0.1375$, GOF = 1.071, largest difference peak/hole 0.66/−0.85 e Å^{-3}. CCDC-230827 (**3b**) contains the supplementary crystallographic data for this paper. These data can be obtained free of charge from The Cambridge Crystallographic Data Centre via www.ccdc.cam.ac.uk/data_request/cif.

Acknowledgements

This work was supported by the Centre National de la Recherche Scientifique and the Ministère de la Recherche et des Nouvelles Technologies (Ph.D. grant to J.-p.T.). M.B. and M.-M.R. thank the IDRIS computer center (Orsay, France). We are grateful to Prof. R. Welter for the X-ray structure determination, Dr D. Mandon for the NIR spectra and Dr M. Bernard and Dr S. Choua (ICS, Strasbourg) for the EPR measurements.

[1] a) C. K. Jørgensen, *Oxidation Numbers and Oxidation States*, Springer, Berlin, **1969**; b) D. Herebian, E. Bothe, E. Bill, T. Weyhermüller, K. Wieghardt, *J. Am. Chem. Soc.* **2001**, *123*, 10012.

[2] For recent examples, see: a) S. Kheradmandan, K. Heinze, H. W. Schmalle, H. Berke, *Angew. Chem.* **1999**, *111*, 2412; *Angew. Chem. Int. Ed.* **1999**, *38*, 2270; b) F. Barigelletti, L. Flamigni, *Chem. Soc. Rev.* **2000**, *29*, 1; c) G. B. Schuster, *Acc. Chem. Res.* **2000**, *33*, 253; d) A. El-ghayouri, A. Harriman, A. Khatyr, R. Ziessel, *Angew. Chem.* **2000**, *112*, 191; *Angew. Chem. Int. Ed.* **2000**, *39*, 185; e) Y. Hoshino, *Platinum Met. Rev.* **2001**, *45*, 2; f) D. Jaganyi, A. Hofmann, R. van Eldik, *Angew. Chem.* **2001**, *113*, 1730; *Angew. Chem. Int. Ed.* **2001**, *40*, 1680; g) J.-P. Launay, *Chem. Soc. Rev.* **2001**, *30*, 386; h) A. Ceccon, S. Santi, L. Orian, A. Bisello, *Coord. Chem. Rev.* **2004**, *248*, 683.

[3] a) C. Creutz, H. Taube, *J. Am. Chem. Soc.* **1969**, *91*, 3988; b) C. Creutz, H. Taube, *J. Am. Chem. Soc.* **1973**, *95*, 1086; c) U. Fürholz, H.-B. Bürgi, F. E. Wagner, A. Stebler, J. H. Ammeter, E. Krausz, R. J. H. Clark, M. J. Stead, A. Ludi, *J. Am. Chem. Soc.* **1984**, *106*, 121; d) S. Joss, H.-B. Bürgi, A. Ludi, *Inorg. Chem.* **1985**, *24*, 949.

[4] See for example: a) F. Paul, C. Lapinte, *Coord. Chem. Rev.* **1998**, *178–180*, 431; b) M. Guillemot, L. Toupet, C. Lapinte, *Organometallics* **1998**, *17*, 1928; c) M. Glöckle, W. Kaim, *Angew. Chem.* **1999**, *111*, 3262; *Angew. Chem. Int. Ed.* **1999**, *38*, 3072; d) M. D. Ward, J. A. McCleverty, *J. Chem. Soc. Dalton Trans.* **2002**, 275; e) L. D. Slep, A. Mijovilovich, W. Meyer-Klaucke, T. Weyhermüller, E. Bill, E. Bothe, F. Neese, K. Wieghardt, *J. Am. Chem. Soc.* **2003**, *125*, 15554; f) F. A. Cotton, C. Y. Liu, C. A. Murillo, X. Wang, *Chem. Commun.* **2003**, 2190; g) A. P. Meacham, K. L. Druce, Z. R. Bell, M. D. Ward, J. B. Keister, A. B. P. Lever, *Inorg. Chem.* **2003**, *42*, 7887; h) P. Gupta, A. Das, F. Basuli, W. S. Sheldrick, H. Mayer-Figge, S. Bhattacharaya, *Inorg. Chem.* **2005**, *44*, 2081; i) S. Kar, B. Sarkar, S. Ghumaan, D. Janardanan, J. van Slageren, J. Fiedler, V. G. Puranik, R. B. Sunoj, W. Kaim, G. K. Lahiri, *Chem. Eur. J.* **2005**, *11*, 4901.

[5] a) M. D. Ward, *Chem. Soc. Rev.* **1995**, *24*, 121; b) A. Aukauloo, X. Ottenwaelder, R. Ruiz, S. Poussereau, Y. Pei, Y. Journaux, P. Fleurat, F. Volatron, B. Cervera, M. Carmen Muñoz, *Eur. J. Inorg. Chem.* **1999**, 1067; c) W. Kaim, A. Klein, M. Glöckle, *Acc. Chem. Res.* **2000**, *33*, 755; d) K. D. Demadis, C. M. Hartshom, T. J. Meyer, *Chem. Rev.* **2001**, *101*, 2655; e) W. Kaim, *Coord. Chem. Rev.* **2002**, *230*, 127.

[6] a) J. Stubbe, W. A. van der Donk, *Chem. Rev.* **1998**, *98*, 705; b) M. Sono, M. P. Roach, E. D. Coulter, J. H. Dawson, *Chem. Rev.* **1996**, *96*, 2841; c) J. S. Miller, A. J. Epstein, *Chem. Commun.* **1998**, 1319; d) H. Iwamura, K. Inoue, N. Koga, *New J. Chem.* **1998**, *22*, 201.

[7] a) M. D. Ward, *Inorg. Chem.* **1996**, *35*, 1712; b) S. Kitagawa, S. Kawata, *Coord. Chem. Rev.* **2002**, *224*, 11; c) C. Carbonera, A. Dei, J.-F. Létard, C. Sangregorio, L. Sorace, *Angew. Chem.* **2004**, *116*, 3198; *Angew. Chem. Int. Ed.* **2004**, *43*, 3136.

[8] a) O. Siri, P. Braunstein, *Chem. Commun.* **2000**, 2223; b) O. Siri, P. Braunstein, M.-M. Rohmer, M. Bénard, R. Welter, *J. Am. Chem. Soc.* **2003**, *125*, 13793; c) M. Elhabiri, O. Siri, A. Sornosa-Tent, A.-M. Albrecht-Gary, P. Braunstein, *Chem. Eur. J.* **2004**, *10*, 134.

[9] C. Kimish, *Ber. Dtsch. Chem. Ges.* **1875**, *8*, 1026.

[10] a) G. C. Allen, N. S. Hush, *Prog. Inorg. Chem.* **1967**, *8*, 357; b) N. Hush, *Prog. Inorg. Chem.* **1967**, *8*, 391.

[11] a) B. Kersting, D. Siebert, *Inorg. Chem.* **1998**, *37*, 3820; b) C. G. Pierpont, L. C. Francesconi, D. Hendrickson, *Inorg. Chem.* **1977**, *16*, 2367; c) A. McAuley, C. Xu, *Inorg. Chem.* **1992**, *31*, 5549; d) A. McAuley, S. Subramanian, *Inorg. Chem.* **1997**, *36*, 5376; e) L. P. Battaglia, A. Bianchi, A. Bonamartini Corradi, E. Garcia-Espana, M. Micheloni, M. Julve, *Inorg. Chem.* **1988**, *27*, 4174; f) S. Brooker, G. B. Caygill, P. D. Croucher, T. C. Davidson, D. L. J. Clive, S. R. Magnuson, S. P. Cramer, C. Y. Ralston, *J. Chem. Soc. Dalton Trans.* **2000**, 3113; g) M. Stollenz, M. Rudolph, H. Görls, D. Walther, *J. Organomet. Chem.* **2003**, *687*, 153; h) G. M. Ferrence, E. Simon-Manso, B. K. Breedlove, L. Meeuwenberg, C. P. Kubiak, *Inorg. Chem.* **2004**, *43*, 1071.

[12] a) User's Guide, Release 1999, Chemistry Department, Vrije Universiteit, Amsterdam (The Netherlands), **1999**; b) E. J. Baerends, D. E. Ellis, P. Ros, *Chem. Phys.* **1973**, *2*, 41; c) G. te Velde, E. J. Baerends, *J. Comput. Phys.* **1992**, *99*, 84; d) C. Fonseca-Guerra, O. Visser, J. G. Snijders, G. te Velde, E. J. Baerends, *Methods and Techniques in Computational Chemistry: METECC-95* (Eds.: E. Clementi, G. Corongiu), STEF: Cagliari, Italy, **1995**, pp. 305–395.

[13] Gaussian 98, revision A.6, M. J. Frisch, G. W. Trucks, H. B. Schlegel, G. E. Scuseria, M. A. Robb, J. R. Cheeseman, V. G. Zakrzewski, J. A. Montgomery, Jr., R. E. Stratmann, J. C. Burant, S. Dapprich, J. M. Millam, A. D. Daniels, K. N. Kudin, M. C. Strain, O. Farkas, J. Tomasi, V. Barone, M. Cossi, R. Cammi, B. Mennucci, C. Pomelli, C. Adamo, S. Clifford, J. Ochterski, G. A. Petersson, P. Y. Ayala, Q. Cui, K. Morokuma, D. K. Malick, A. D. Rabuck, K. Raghavachari, J. B. Foresman, J. Cioslowski, J. V. Ortiz, B. B. Stefanov, G. Liu, A. Liashenko, P. Piskorz, I. Komaromi, R. Gomperts, R. L. Martin, D. J. Fox, T. Keith, M. A. Al-Laham, C. Y. Peng, A. Nanayakkara, C. Gonzalez, M. Challacombe, P. M. W. Gill, B. G. Johnson, W. Chen, M. W. Wong, J. L. Andres, M. Head-Gordon, E. S. Replogle, J. A. Pople, Gaussian, Inc, Pittsburgh, PA, **1998**.

[14] a) O. Gritsenko, E. J. Baerends, *J. Chem. Phys.* **2004**, *121*, 655; b) A. Dreuw, M. Head-Gordon, *J. Am. Chem. Soc.* **2004**, *126*, 4007; c) S. Grimme, M. Parac, *ChemPhysChem* **2003**, *4*, 292.

[15] a) N. D. J. Branscombe, A. J. Atkins, A. Marin-Beccera, E. J. L. McInnes, F. E. Mabbs, J. McMaster, M. Schröder, *Chem. Commun.* **2003**, 1098; b) T. Ito, N. Imai, T. Yamaguchi, T. Hamaguchi, C. H. Londergan, C. P. Kubiak, *Angew. Chem.* **2004**, *116*, 1400; *Angew. Chem. Int. Ed.* **2004**, *43*, 1376; c) Y. Shimazaki, F. Tani, K. Fukui, Y. Naruta, O. Yamauchi, *J. Am. Chem. Soc.* **2003**, *125*, 10512.

[16] a) D. Walther, T. Döhler, N. Theyssen, H. Görls, *Eur. J. Inorg. Chem.* **2001**, 2049; b) D. Zhang, G.-X. Jin, *Organometallics* **2003**, *22*, 2851.

[17] R. H. Blessing, *Crystallogr. Rev.* **1987**, *1*, 3.

[18] G. M. Sheldrick, SHELXL97, Program for the refinement of crystal structures, University of Göttingen (Germany), **1997**.

Received: March 14, 2005
Revised: June 20, 2005
Published online: September 27, 2005

